Reentrant smectic-C and smectic-C^* phases in liquid crystals under an electric field

L. Benguigui
Solid State Institute and Department of Physics, Technion, Haifa 32000, Israel

A.E. Jacobs*
Department of Physics, Tokyo Institute of Technology, Oh-okayama, Meguro-ku, Tokyo 152, Japan
(Received 8 September 1993; revised manuscript received 22 December 1993)

Kondo *et al.* [Jpn. J. Appl. Phys. **22**, L43 (1983)] discovered that both the smectic-C and smectic-C^* phases in the liquid crystal p-n-decyloxybenzylidene-p-amino-2-methylbutyl-cinnamate are reentrant with temperature for a range of electric fields. We show that the Landau theory with no adjustable parameters provides a semiquantitative explanation of the phase diagram. The double reentrance is due to two fourth-order terms, one chiral and the other achiral, and is intimately related to the maximum in the pitch, unlike the reentrance under magnetic field. The Sm-C–Sm-C* transition curve displays both main types of second-order phase transition, instability, and nucleation, separated by a first-order segment. p-azoxy-cinnamate-methyl-2-butanol and other compounds with divergent pitch should also show the double reentrance, but the physical origin is different.

PACS number(s): 61.30.Cz, 83.70.Jr, 64.70.Md, 77.80.Bh

I. INTRODUCTION

The smectic phases of liquid crystals have layered structures with positional order in the direction normal to the planes. There are three principal phases. In the smectic-A (Sm-A) phase, the molecules are parallel on average to the layer normal. In the smectic-C (Sm-C) phase, the molecular director is tilted, making an angle θ with the normal. In the smectic-C^* (Sm-C^*) phase, the molecules are again tilted; the structure is helical, with the helix axis perpendicular to the layers (the azimuthal angle ϕ of the projection of the director onto the layer planes rotates with the coordinate along the normal). A typical phase sequence with decreasing temperature for a nonracemic mixture of chiral molecules is isotropic→Sm-A →Sm-C^* (in zero field).

Interest in smectic phases was greatly stimulated by the discovery [1] of ferroelectric liquid crystals. If the molecules possess an electric dipole moment with a component normal to the director, the tilt in the Sm-C and Sm-C^* phases hinders molecular rotation about the long axis, producing a spontaneous electric polarization (parallel to the layers and perpendicular to the director). The macroscopic polarization vanishes in the Sm-C^* phase, but an electric or a magnetic field parallel to the layers distorts the helicoidal structure, disfavoring the Sm-C^* phase, and leading eventually to the Sm-C phase which has a macroscopic polarization.

The Sm-C→Sm-C^* transition under *magnetic* field was first observed by Muševič *et al.* [2], in the liquid crystal p-n-decyloxybenzylidene-p-amino-2-methylbutyl-cinnamate (DOBAMBC); they found the Sm-A—Sm-C–Sm-C^* Lifshitz point which had been predicted by Michelson [3], but observed (unexpectedly) that the Sm-C^* phase is reentrant: for a range of fields, the phase transitions Sm-A →Sm-C^*→Sm-C →Sm-C^* occur with decreasing temperature. The reentrance of the Sm-C^* phase was explained in Refs. [4] and [5].

Early experiments under *electric* field found a monotonic decrease of the critical temperature with increasing field, for DOBAMBC [6], for several members of the DOBAMBC family [7] (see Fig. 25; but some results on DOBAMBC suggest reentrance—see Fig. 26 and the discussion in [7]), and for 2-methylbutyl-p-(p-n-hexyloxybenylizene-amino)-cinnamate [8] (but the pitch varied unexpectedly rapidly). Later experiments gave different results; the samples are difficult both to prepare and to measure (many of the compounds are unstable at elevated temperature), and properties vary markedly. Shortly after the work of Muševič *et al.* [2], Kondo *et al.* [9,10] (examining the DOBAMBC family) observed the phase sequence Sm-C^*→Sm-C →Sm-C^* with decreasing temperature for a range of fields; strictly speaking, only Sm-C^* reentrance was observed, but the Sm-A and Sm-C phases have the same symmetry in an electric field and so the Sm-C phase must also be reentrant, giving a nice parallel with the magnetic-field case [2]. Subsequent experiments on DOBAMBC found reentrance [11], hysteresis, and an apparent divergence in the pitch (but not literal reentrance) [12] and both reentrance and hysteresis [13]. Reentrance and hysteresis were observed in p-decycloxybenzylidene-p'-amino-1-methylpropyl-cinnamate (DOBA-1-MPC) [14] and reentrance in (S)-2-hydroxy-4-decyloxybenzylidene-4′-amino-2p''-methylbutyl-cinnamate [15]. At least two different geometries are used in the experiments, planar and homeotropic; the first favors reentrance and hysteresis [7].

Section II reviews previous work on the Landau theory of the Sm-C–Sm-C^* transition in the presence of an electric field and also some experimental results. Section III analyzes a simple free-energy density (which applies to some samples), using both approximate and numerical solutions of the Euler-Lagrange equations. Section IV compares the theoretical and experimental E-T phase diagrams of DOBAMBC, finding reasonable agreement,

*Present and permanent address: Department of Physics, University of Toronto, Toronto, Ontario, Canada M5S 1A7.

all that can be expected given the variance of the experimental results and the neglect of terms in the theory. The double reentrance in DOBAMBC is due to the combined action of the chiral term responsible for the reentrance under magnetic field and the achiral term linked to the maximum in the pitch at zero field. Finally, Sec. V discusses various possibilities for the phase diagrams under electric or magnetic field and suggests further experiments.

II. FREE-ENERGY DENSITY

In the Landau theory of smectic liquid crystals under electric field [1,16–20], the free-energy density $\mathcal{F}$ is expanded in primary and secondary order parameters, the projection $\mathbf{n} = (n_x, n_y)$ of the director onto the layer plane, and the layer polarization $\mathbf{P} = (P_x, P_y)$, respectively; we take the layer normal in the z direction:

$$\mathcal{F} = \frac{A}{2}(n_x^2 + n_y^2) + \frac{B}{4}(n_x^2 + n_y^2)^2 + \frac{C}{6}(n_x^2 + n_y^2)^3 + D_1\left[\left(\frac{dn_x}{dz}\right)^2 + \left(\frac{dn_y}{dz}\right)^2\right]$$
$$-D_2\left(n_x\frac{dn_y}{dz} - n_y\frac{dn_x}{dz}\right) + \frac{1}{2\chi}(P_x^2 + P_y^2) + k(P_x n_y - P_y n_x) - \mu\left(P_x\frac{dn_x}{dz} + P_y\frac{dn_y}{dz}\right) - \mathbf{P}\cdot\mathbf{E}$$
$$-D_3\left(n_x^3\frac{dn_y}{dz} - n_y^3\frac{dn_x}{dz}\right) - \frac{\Omega}{2}(P_x n_y - P_y n_x)^2 + \frac{\eta}{4}(P_x^2 + P_y^2)^2 \; ; \qquad (1)$$

we omit a term (quadratic in the electric field) which is known to be small [21,22].

As usual, only the coefficient A depends on the temperature T: $A = A'(T - T_0)$; the Sm-A–Sm-C^* transition in zero field occurs at a temperature $T_c(0)$ greater than T_0. The D_1 term is the elastic energy ($D_1 = K_3/2$) and the chiral D_2 term (a Lifshitz invariant) is primarily responsible for the Sm-C^* phase; the k and μ terms are chiral, piezoelectric and achiral, flexoelectric in nature. The last three terms (with coefficients D_3, Ω, and η) have no effect on the Sm-A–Sm-C and Sm-A–Sm-C^* phase boundaries under magnetic field; their effect is small on the Sm-C–Sm-C^* boundary both near the Lifshitz point in magnetic field and for small electric field [where the result [16] $T_c(E) = T_c(0) - \alpha E^2$ is generally valid, as observed in the early experiments [6–8]].

If the last two terms (with coefficients Ω and η) in Eq. (1) can be neglected, then the polarization can be eliminated by $\mathbf{P} = \chi(\mathbf{E} + k\hat{\mathbf{z}} \times \mathbf{n} + \mu d\mathbf{n}/dz)$; the other four terms depending on $\mathbf{P}$ are replaced by a constant, and one obtains an expansion in $\mathbf{n}$ alone, with some coefficients renormalized. In zero field, the solution for $\mathbf{n}$ is $(n_x, n_y) = n(\cos qz, \sin qz)$, with $\mathbf{P}\cdot\mathbf{n} = 0$; the ratio P/n is independent of T (the amplitudes P and n are "proportional") and the pitch $p = 2\pi/q$ changes monotonically with T (that is, the ratio P/n can be independent of T even if the pitch depends on T). If in addition the coefficient D_3 is small, then the pitch is also independent of T.

In most DOBAMBC samples both the pitch p and the ratio P/n depend significantly on T. The pitch has a maximum, while P/n is approximately constant if $T \lesssim T_c - 2\text{K}$ but decreases sharply as $T \to T_c$ (by roughly a factor of 2) [23]. (Reference [23] discusses the ratio P/θ, but θ and $n = \sin\theta$ are almost equal near the transition.) To explain these results, both the chiral D_3 term and the achiral Ω term must be included in Eq. (1) (and therefore also the η term, for stability). The maximum in p at zero field arises as follows: the Ω term favors the spatially homogeneous Sm-C phase, increasingly enhances its stability with decreasing T and causing p to increase initially with decreasing T; the D_3 term favors the inhomogeneous Sm-C^* phase ($D_2 D_3 > 0$ for DOBAMBC) and eventually causes p to decrease, giving the maximum. Other explanations of the maximum have been given [24–26].

The reentrance of the Sm-C^* phase has been attributed to fluctuations (thermal generation of antisolitons [27]), but the wide variety of observed behavior [28] argues against this interpretation. References [4] and [5] showed that the chiral D_3 term in Eq. (1) is responsible for the reentrance of the Sm-C^* phase under magnetic field H (this term is the product of the two invariants with coefficients A and D_2, apart from a factor and a surface term). A qualitative explanation follows: Near the Lifshitz point, dT_c/dH (T_c is the Sm-C–Sm-C^* transition temperature) is always positive, regardless of the zero-field behavior of the pitch [3]. Without the D_3 term, the critical magnetic field H_c is independent of T at low T; if $D_2 D_3 > 0$, the D_3 term (optimized by the Sm-C^* phase) shifts the phase boundary to ever larger H with decreasing T. The combination of the conditions $dT_c/dH > 0$ near the Lifshitz point and $dT_c/dH < 0$ at low T gives the reentrance. By itself, the Ω term cannot give a reentrant Sm-C^* phase (which reflects enhanced stability of this phase), only a reentrant Sm-C phase. The double reentrance under electric field requires both terms (D_3 and Ω).

The density of Eq. (1) is distastefully complicated, but all terms have received a microscopic explanation and all are necessary to provide a semiquantitative description of materials such as DOBAMBC (for which all parameters have been determined). But Eq. (1) is not a systematic expansion in the order parameters to given order (it omits terms of the same order as those retained) and it is therefore unreasonable to expect the theory to explain quantitatively all phenomena; indeed the fits to the pitch are only semiquantitative.

III. THE CASE OF ONE ORDER PARAMETER

We consider the simple case with only one order parameter, choosing **P** as in Ref. [17]; the free-energy density is

$$\mathcal{F} = \frac{A}{2}\left(P_x^2 + P_y^2\right) + \frac{B}{4}\left(P_y^2 + P_y^2\right)^2 + \frac{C}{6}\left(P_y^2 + P_y^2\right)^3 + D_1\left[\left(\frac{dP_x}{dz}\right)^2 + \left(\frac{dP_y}{dz}\right)^2\right] - D_2\left(P_x\frac{dP_y}{dz} - P_y\frac{dP_x}{dz}\right) - D_3\left(P_x^3\frac{dP_y}{dz} - P_y^3\frac{dP_z}{dz}\right) - \mathbf{P}\cdot\mathbf{E}\ . \quad (2)$$

A similar expression was studied in our previous work on magnetic-field unwinding [4,5], where we expanded naturally in **n**. The coefficients differ of course from those in Eq. (1). Equation (2) appears to describe the DOBAMBC samples of Ref. [7], where the pitch decreases with decreasing T (or the maximum occurs unobservably close to T_c), but not the DOBAMBC samples of Refs. [9,10,2,22] and others.

In the one-harmonic approximation (valid at high T), we write $P_x = P\cos qz + P_0$, $P_y = P\sin qz$ and minimize the free energy with respect to the parameters q, P, and P_0; **E** is parallel to the x axis. Reference [17] showed that it is a good approximation to take the induced polarization P_0 to be independent of z, but strictly P_0 depends on z even if the electric field is uniform [29]. Because the problem is nonlinear, P_0 is not necessarily proportional to E, as sometimes assumed [7,14].

In the constant-amplitude approximation (valid at low T and used frequently [1,18,21,14]), we assume that $\mathbf{P} = P[\cos\phi(z), \sin\phi(z)]$, and look for the constant P and the function $\phi(z)$ which minimize the free energy. Standard calculations (such as those for the unwinding of cholesterics [30]) give the wave number q and the critical field E_c as

$$q = \frac{D_2}{2D_1}\left(1 + \frac{3}{4}\frac{D_3}{D_2}P^2\right)\ , \quad (3)$$

$$E_c = \frac{\pi^2}{8}D_1 P q^2\ , \quad (4)$$

with P^2 given by $A + BP^2 + CP^4 = 0$. Equation (3) is familiar from Refs. [20,4,5]; if P and n are proportional, then Eq. (4) follows also from the relation [1] $E_c = (\pi^2/16)K_3 n^2 q^2/P$.

Equation (4) may be valid also when n and P are not proportional. From the solutions $\mathbf{n}(z)$ and $\mathbf{P}(z)$ of the Euler-Lagrange equations for the density of Eq. (1), it is always possible, in principle, to express **n** as a function of **P**. Elimination of **n** from the density will give a functional depending only on **P** (and its derivatives). Because of the symmetry, the new functional will have the same form as Eq. (2) (with maybe other terms, but their presence will not change the conclusion) with an important difference: the coefficients (which were previously supposed to have a negligible temperature dependence, except A) are now functions of T and also E. This will not change the result of the constant-amplitude approximation and the critical field is still given by Eq. (4), if the dependence on E is weak.

A plot (Fig. 1) of E_c/n against q^2 for the DOBAMBC and *p*-octyloxybenzylidene-*p'*-amino-2-methylbutyl-α-methyl-cinnamate (OOBAMBMC) samples of Ref. [7] confirms the validity of Eq. (4) and also our assumption that $P \propto n$ for these samples; note that we plot E_c/n, not E_c/P. Another point is that the constant-amplitude approximation seems to be valid over a large temperature range, except for $T \gtrsim T_c(E) - 1$ K; see also Figs. 3 and 4 below. Figure 2 plots E_c against Pq^2 for the DOBAMBC samples of Refs. [9] and [10]. The observed linear relation [as predicted by Eq. (4)] means that the coefficient D_1 is practically independent of T; this result, which cannot be predicted theoretically, permits the use of Eq. (4) even in cases where the simple derivation given above does not apply.

We discuss next the numerical solution of the Euler-Lagrange equations for the density of Eq. (2); there are six parameters (and also the unknown temperature T_0), but scaling the polarization, the length scale, and the free energy reduces this number to three. Since we are interested here only in the qualitative features of the phase diagram in the E-A plane, we have used an illustrative parameter set ($B = 200$, $C = 3000$, $D_1 = 1$, and $D_2 = 2$, with $D_3 = 0$ or 10 or -10). We note that the chiral D_2 and D_3 terms in the free-energy density can either co-

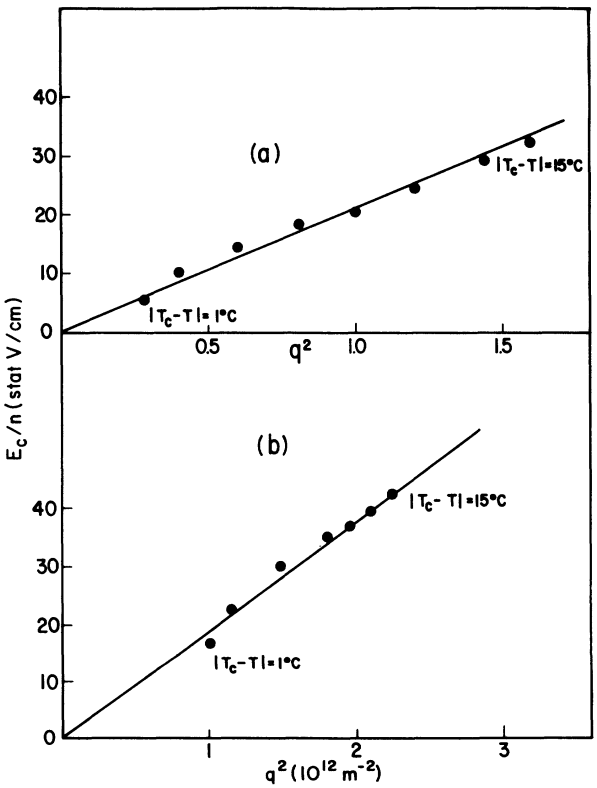

FIG. 1. Plot of E_c/n vs q^2 for two compounds studied by Martinot-Lagarde *et al.* [7]: (a) DOBAMBC and (b) OOBAMBMC.

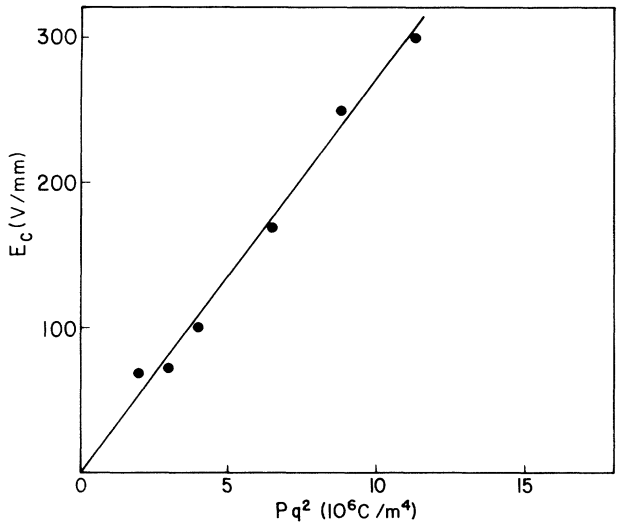

FIG. 2. Plot of E_c vs Pq^2 for the DOBAMBC samples of Takezoe *et al.* [10].

operate ($D_2D_3 > 0$) or compete ($D_2D_3 < 0$), favoring helices with the same sense of rotation or opposite senses respectively, with consequences for the phase diagram.

Figure 3, which gives the results of numerical solution of the Euler-Lagrange equations for $D_3 = 0$ and $D_3 = 10$, shows that the critical electric field depends monotonically on T. The D_3 term merely displaces the transition to larger electric field (since $D_2D_3 > 0$); in a *magnetic* field, on the other hand, the D_3 term makes the Sm-C^* phase reentrant [4,5]. The two approximations used together provide an excellent description of the phase diagram for $D_3 = 10$; see also Fig. 4 below.

Figure 4 shows the phase diagram for the same parameter values, except that $D_3 = -10$. The D_2 and D_3 terms compete, the first winning at high T where n is small and the second at low T (but this region may not be experimentally accessible due to the appearance of other phases). The helix reverses sense at some T less than T_c (the wave number vanishes and the pitch diverges), giving the doubly reentrant sequence Sm-C →Sm-C^*→Sm-C →Sm-C^* with decreasing T (for a range of fields). Compounds such as PACMB [7], in which the helix unwinds completely with decreasing T and then rewinds in the other direction (at zero field), should show a phase diagram like Fig. 4.

In all three cases ($D_3 = -10$, 0, and 10 in Figs. 3 and 4), the transition at high T is second order (instability type), switches to first order, and then to second order (nucleation type). This is the only case known to us where both main types of second-order transition occur on the same phase boundary; the first-order segment is necessary to separate them. The upper multicritical point was predicted in Ref. [17]; on the second-order line above this point, the Sm-C phase becomes unstable to a ripple. At the lower multicritical point, the interaction between discommensurations changes from attractive to repulsive [5,31].

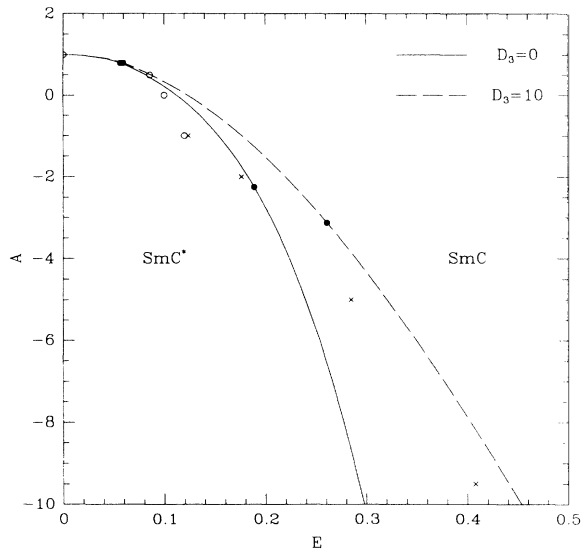

FIG. 3. Phase diagram in the E-A plane for the Landau density of Eq. (2), with parameters $B = 200$, $C = 3000$, $D_1 = 1$, $D_2 = 2$, and $D_3 = 0$ (solid line) and 10 (dashed line). The smectic-C^* (Sm-C^*) and smectic-C (Sm-C) phases occur at low and high fields, respectively. The •'s are multicritical points separating second-order transitions at high and low temperatures (instability and nucleation types, respectively) from first-order transitions at intermediate temperatures. The o's and ×'s are the results of the one-harmonic and constant-amplitude approximations for $D_3 = 10$.

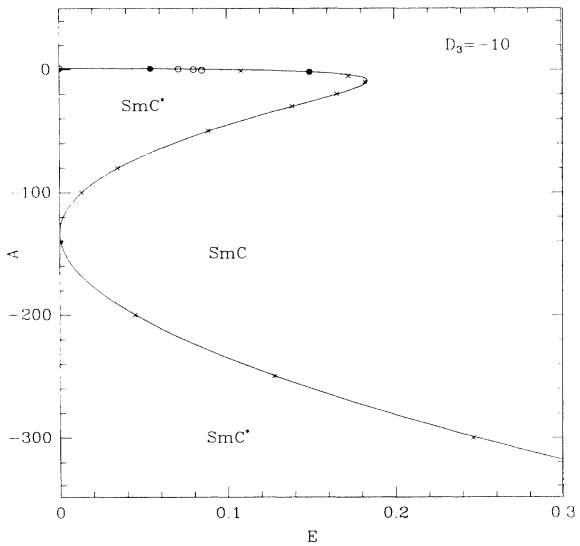

FIG. 4. Phase diagram in the E-A plane for the Landau density of Eq. (2), with parameters $B = 200$, $C = 3000$, $D_1 = 1$, $D_2 = 2$, and $D_3 = -10$. The helices of the smectic-C^* phases in the two regions have opposite senses. The •'s are the multicritical points; the other points are the results of the one-harmonic approximation (o's), and the constant-amplitude approximation (×'s). The figure should describe qualitatively the phase diagram of PACMB [7] and other compounds with divergent pitch at zero field.

IV. PHASE DIAGRAM OF DOBAMBC

This section compares the theoretical E-T phase diagram of DOBAMBC [obtained by numerical solution of the Euler-Lagrange equations corresponding to the density of Eq. (1)] with experiment. Unfortunately, DOBAMBC samples can have very different properties when prepared in different laboratories and the two available sets of parameters (the "A" set of Ref. [22] and the "Carlsson set" [32]) differ markedly, in cases by several orders of magnitude, although both sets gave good fits for $n(T)$, $P(T)$, and the ratio P/n, and semiquantitative fits for the pitch; E-T phase diagrams were not used to estimate the parameters and in fact were not determined for these samples. No full sets of parameter values are available for the samples used to determine the phase diagrams. The Carlsson set gives better agreement with experiment, but we have no other evidence to prefer it. Only an incomplete parameter set is available for DOBA-1-MPC [33].

Figure 5 compares the phase diagram predicted by the Carlsson set with the experimental results of Ref. [10]. We emphasize that the theoretical phase diagram was obtained from numerical solution of the Euler-Lagrange equations for the density of Eq. (1), using no adjustable parameters, only published values obtained from fits to experimental results (which do not include the phase diagram). Experimental values of the field at the left nose are $E = 64$ V/mm [10], ~70 V/mm [11], ~58 V/mm ([13], decreasing field), and ~79 V/mm ([13], increasing field), in good agreement with our numerical value of 69 V/mm (at $T - T_0 = -1.8$ K). The right nose (which occurs at $E = 172$ V/mm, $T - T_0 = -0.31$ K numerically) and the upper branch were not observed in any of the experiments on DOBAMBC [10,11,13], apparently because measurements very near T_c are too difficult. Also, the phase boundary at low T turns downward experimentally [10] but upward numerically, perhaps due to sample differences (between those of Refs. [10] and [32]) or (less likely) due to terms omitted in the Landau theory. Apart from these qualifications, the overall agreement is satisfactory, considering that (a) the experimental properties vary greatly (and so do the parameter values), (b) parameter values are not available for the samples used to determine the phase diagram, and (c) the available parameters give only semiquantitative fits.

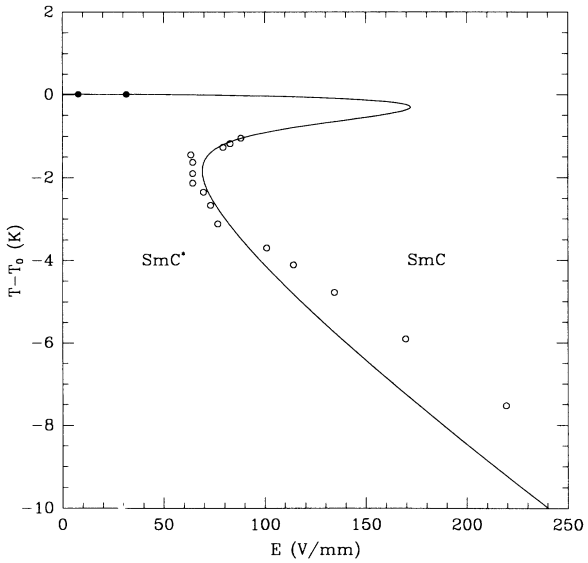

FIG. 5. Phase diagram in the E-T plane as predicted by the Landau density of Eq. (1) with the Carlsson set of parameter values [32] for DOBAMBC. The solid circles are the multicritical points discussed in the caption for Fig. 3. The o's are the experimental points from Fig. 13 of Takezoe *et al.* [10]. One experimental point at large field is not plotted; the transition temperature at zero field was not measured, and we have adjusted the experimental points so that the highest one lies on the theoretical curve.

The transition is predicted to be second order except between the multicritical points. The first order segment is probably unobservable because it occurs in the difficult high-T region; more generally, the commensurate-incommensurate transition in systems of the Lifshitz-invariant class, when first order, is only weakly so, with little hysteresis. The order is difficult to determine experimentally, but a second-order transition is not inconsistent [34] with the results of Ref. [10]. The hysteresis observed in some experiments [12–14] suggests a first-order transition (in disagreement with the theory), but may be due to sample geometry, or difficulty in reaching equilibrium [35].

We determined the phase diagram also for the "A" parameter set of Ref. [22]. The double reentrance occurs for this set as well; the left and right noses are at $(E, T - T_0) = (21$ V/mm, -0.12 K) and (2.5 V/mm, -3.0 K), in poor agreement with the available E-T phase diagrams.

Parameters for weakly chiral DOBAMBC samples were obtained by fitting to the H-T phase diagram [35]; values of three of the six adjustable parameters differ significantly from those obtained previously, partly because the earlier fit [32] was to chiral samples. The fit at low T was good, but not in the difficult high-T region; also, Ref. [35] did not examine whether other properties are well described by these parameters. Similar calculation of the H-T phase diagram of chiral samples using the chiral set [32] would be of interest.

The left nose of the E-T phase diagram, but not the right nose or the upper branch, can be understood simply from a relation giving the critical field in terms of measured quantities:

$$E_c \approx \frac{\pi^2}{32}\frac{P_s}{P_i/E}\ , \tag{5}$$

where P_s and P_i are the spontaneous and induced polarizations, the latter being assumed linear in the field E. Applications to DOBAMBC and DOBA-1-MPC are given in Ref. [14] where Eq. (5) was first given; it is obtained on combining Eqs. (25), (44), and (45) of Ref. [18], apart from a factor of $\pi^2/8$.

The double reentrance in DOBAMBC under electric field [9–11,13] is unusual, as is the Sm-C^* reentrance under magnetic field [2], deserving a few comments. A nonracemic mixture of chiral molecules is obviously necessary, but not sufficient.

A. Electric field

In the cooperative case $D_2D_3 > 0$, the double reentrance, like the maximum in the pitch, requires both the chiral D_3 term and the achiral Ω term. In colloquial terms, the Ω term creates the right nose, making the Sm-C phase reentrant, and the D_3 term creates the left nose, making the Sm-C^* phase also reentrant. But the Ω term alone can give a reentrant Sm-C phase without a reentrant Sm-C^* phase, as shown in Fig. 6. In the competitive case $D_2D_3 < 0$, only the D_3 term is needed for the double reentrance.

B. Magnetic field

In colloquial terms, the Lifshitz point in magnetic field plays the role of the right nose in electric field, giving the phase boundary in the H-T plane a positive slope; the D_3 term (in the cooperative case) enhances the Sm-C^* stability with decreasing T, and turns the curve around, causing the reentrance. Compounds without a maximum in the pitch can have a reentrant Sm-C^* phase, as shown in our previous work [4,5] [which omitted the Ω and η terms in Eq. (1)]; the reentrance may be more common than realized and failure to observe the maximum should not discourage experiments in magnetic field. Of course a quantitative description of the phase boundary may require the Ω term. The theory is quite clear on the relation between the maximum in the pitch and the reentrance, unlike some of the literature [35]; it is not the maximum but rather the decrease of p with decreasing T, which is connected to the reentrance.

V. SUMMARY

The following, together with Fig. 7, gives the expected behavior under magnetic (H) or electric (E) field according to the behavior of the pitch p with decreasing T; we use this quantity as a guide because it measures the sizes of the crucial D_3 and Ω terms. We note the present experimental situation, and suggest further experiments, but caution that the appearance of other phases may preempt the predicted reentrance. The list is not exhaustive: more complicated behavior is possible, as are intermediate cases [such as MHPOOCBC (the chemical formula is given in Ref. [28])].

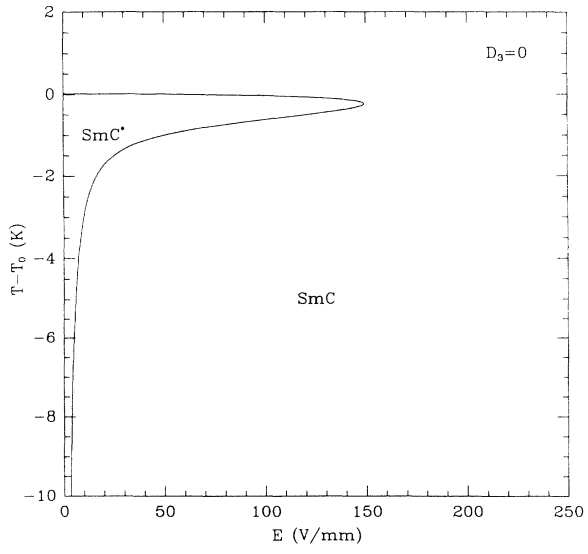

FIG. 6. Phase diagram in the E-T plane as predicted by the Landau density of Eq. (1) with the Carlsson set of parameter values [32], except that $D_3 = 0$.

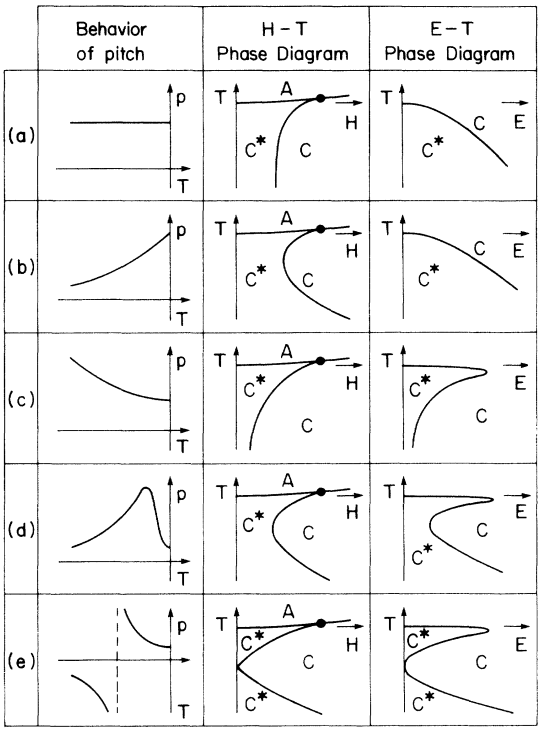

FIG. 7. Some possible behaviors of the pitch p as a function of T with the corresponding H-T and E-T phase diagrams. Of the six cases showing reentrance, only two (line D under H and under E) have been observed experimentally; the text suggests compounds which may display the other four.

(a) The pitch is constant. Both D_3 and Ω are small; neither the Sm-C nor the Sm-C^* phase is reentrant under either H or E.

(b) The pitch decreases monotonically. Ω is small; the Sm-C^* phase is reentrant under H; neither phase is reentrant under E. The DOBAMBC samples of Ref. [7] appear to belong to this class, but the H-T phase diagram was not determined. Observation of Sm-C^* reentrance without a maximum in p would confirm the analysis at the end of Sec. IV.

(c) The pitch increases monotonically. D_3 is small; neither phase is reentrant under H; the Sm-C phase is reentrant under E. MHPOOCBC might belong to this class, but the pitch tends to saturate after an initial rapid increase [28], with a net increase of about 80% above the value at T_c. For comparison, the pitch for the results in Fig. 6 increases by less than 20% at the nose; it does not saturate. That is, the Ω term may be large enough in MHPOOCBC to give reentrance.

(d) The pitch has a maximum. Both terms are large; the Sm-C^* phase is reentrant under H, as observed in

DOBAMBC [2]; both phases are reentrant under E, as observed in DOBAMBC [9,10] and in DOBA-1-MPC [14].

(e) The pitch diverges. This is the competitive case $D_2D_3 < 0$, with $|D_3|$ large; the Sm-C^* phase is reentrant under H and both phases are reentrant under E [as in case (d), but the physical origin is different here, since the Ω term is not required]. The compound p-azoxy-cinnamate-methyl-2-butanol is an example [7], but has not been examined under either magnetic or electric field to our knowledge. The pitch appears to diverge also in the antiferroelectric Sm-C_A^* phase of 4-(1-methylheptyloxycarbonyl)-phenyl-4′-octyloxybiphenyl-4-carboxylate [28], but the above Landau theory requires adjustment, and we cannot predict reentrance under magnetic field.

In conclusion, Landau theory describes reasonably well the phase diagram of DOBAMBC under electric field, an addition to its already impressive list of triumphs in describing the unusual behavior of ferroelectric liquid crystals. Determination of (1) the E-T phase diagram of samples with increasing pitch, (2) the H-T phase diagram of samples with decreasing pitch, and (3) both phase diagrams of samples with diverging pitch, would further test it.

ACKNOWLEDGMENTS

We are grateful to Professor H. Takezoe for informing us of the reentrance under an electric field and for valuable discussions of the experimental results. This research was sponsored by the Japan Society for the Promotion of Science and the Natural Sciences and Engineering Research Council of Canada.

[1] R.B. Meyer, L. Liébert, L. Strzelecki, and P. Keller, J. Phys. Lett. (Paris) **36**, L69 (1975).
[2] I. Muševič, B. Žekš, R. Blinc, Th. Rasing, and P. Wyder, Phys. Rev. Lett. **48**, 192 (1982).
[3] A. Michelson, Phys. Rev. Lett. **39**, 464 (1977).
[4] L. Benguigui and A.E. Jacobs, Ferroelectrics **84**, 379 (1988).
[5] A.E. Jacobs and L. Benguigui, Phys. Rev. A **39**, 3622 (1989).
[6] H. Takezoe, K. Furuhata, T. Nakagiri, A. Fukuda, and E. Kuze, Jpn. J. Appl. Phys. **17**, 1219 (1978).
[7] Ph. Martinot-Lagarde, R. Duke, and G. Durand, Mol. Cryst. Liq. Cryst. **75**, 249 (1981).
[8] K. Kondo, Y. Sato, H. Takezoe, A. Fukuda, and E. Kuze, Jpn. J. Appl. Phys. **20**, L871 (1981).
[9] K. Kondo, H. Takezoe, A. Fukuda, and E. Kuze, Jpn. J. Appl. Phys. **22**, L43 (1983).
[10] H. Takezoe, K. Kondo, K. Miyasato, S. Abe, T. Tsuchiya, A. Fukuda, and E. Kuze, Ferroelectrics **58**, 55 (1984).
[11] S.A. Różański and W. Kuczyński, Chem. Phys. Lett. **105**, 104 (1984).
[12] S. Kai, M. Takata, and K. Hirakawa, Jpn. J. Appl. Phys. **22**, 938 (1983).
[13] S. Dumrongrattana and C.C. Huang, J. Phys. (Paris) **47**, 2117 (1986).
[14] A. Levstik, Z. Kutnjak, B. Žekš, S. Dumrongrattana, and C.C. Huang, J. Phys. II (Paris) **1**, 797 (1991).
[15] A. Ezcurra *et al.*, Liq. Cryst. **4**, 125 (1989).
[16] A. Michelson, L. Benguigui, and D. Cabib, Phys. Rev. A **16**, 394 (1977).
[17] A. Michelson and D. Cabib, J. Phys. Lett. (Paris) **38**, L321 (1977).
[18] S.A. Pikin and V.L. Indenbom, Usp. Fiz. Nauk **125**, 251 (1978) [Sov. Phys. Usp. **21**, 487 (1978)].
[19] C.C. Huang and J.M. Viner, Phys. Rev. A **25**, 3385 (1982); R.J. Birgeneau *et al.*, *ibid.* **27**, 1251 (1983); M. Meichle and C.W. Garland, *ibid.* **27**, 2624 (1983); S.C. Lien, C.C. Huang, and J.W. Goodby, *ibid.* **29**, 1371 (1984); T. Carlsson and I. Dahl, Mol. Cryst. Liq. Cryst. **95**, 373 (1983); S.C. Lien *et al.*, *ibid.* **108**, 148 (1984); J. Theon and G. Seynhaeve, *ibid.* **127**, 229 (1985).
[20] B. Žekš, Mol. Cryst. Liq. Cryst. **114**, 259 (1984).
[21] Ph. Martinot-Lagarde, Mol. Cryst. Liq. Cryst. **66**, 61 (1981).
[22] C.C. Huang and S. Dumrongrattana, Phys. Rev. A **34**, 5020 (1986). We use the authors' parameter set A, fitted to the data of S. Dumrongrattana *et al.*, Phys. Rev. A **34**, 5010 (1986) and of B.I. Ostrovskii *et al.*, Zh. Eksp. Teor. Fiz. **74**, 1748 (1978) [Sov. Phys. JETP **47**, 912 (1978)], as quoted in Ref. [32].
[23] S. Dumrongrattana and C.C. Huang, Phys. Rev. Lett. **56**, 464 (1986).
[24] M.A. Osipov and S.A. Pikin, Zh. Eksp. Teor. Fiz. **82**, 774 (1982) [Sov. Phys. JETP **55**, 458 (1983)].
[25] M. Yamashita and H. Kimura, J. Phys. Soc. Jpn. **51**, 2419 (1982).
[26] M. Nakagawa, Liq. Cryst. **3**, 573 (1988).
[27] M. Yamashita and H. Kimura, J. Phys. Soc. Jpn. **52**, 333, (1983); **52**, E712 (1983); **52**, 1509 (1983).
[28] J. Li, H. Takezoe, and A. Fukuda, Jpn. J. App. Phys. **30**, 532 (1991).
[29] L. Benguigui, Ferroelectrics **58**, 269 (1984).
[30] P.G. de Gennes, Solid State Commun. **6**, 163 (1968).
[31] A.E. Jacobs and M.B. Walker, Phys. Rev. B **21**, 4132 (1980).
[32] T. Carlsson, B. Žekš, C. Filipič, A. Levstik, and R. Blinc, Mol. Cryst. Liq. Cryst. **163**, 11 (1988).
[33] C.C. Huang, S. Dumrongrattana, G. Nounesis, J.J. Stofko, Jr., and P.A. Arimilli, Phys. Rev. A **35**, 1460 (1987).
[34] H. Takezoe (private communication).
[35] B. Kutnjak-Urbanc and B. Žekš, Phys. Rev. E **48**, 455 (1993).